Investigation on High Power Laser Removal of Thermal Barrier Coating (TBC) and Bond Layer (MCrAlY) from Inconel 718 Alloy

J. C. Hernandez-Castaneda, W. Y. Chi, F. Yongwei, Ng F. Lan,
M. C. C. Khin and Z. Hongyu[*]

[1]*Singapore Institute of Manufacturing Technology, 2 Fusionopolis Way, #08-04, Innovis, 138634, Singapore*
[2]*School of Mechanical Engineering, Shandon University of Technology, Zibo, Shandong, China*

This paper reports the development of a precise laser removal process of thermal barrier coating (TBC) and bond layer (BL) from aero engine components as an alternative method to hazardous chemical bath processes. A high power Nd:YAG laser (λ=1064 nm, τ=38 ns) system was successfully employed to remove yttria-stabilised zirconia (TBC) coating and bond layer (MCrAlY) from equiaxial grain Inconel 718 alloy. Investigation on the different assisting media and process conditions to remove TBC coating by high power pulsed laser are reported. A parametric investigation of direct laser removal process of the TBC coating established optimal conditions to achieve 140 mm³/min removal rate. A novel two-step laser scanning method was developed to remove the bond layer coating at 10 mm³/min and with a minimal recast layer of 4 μm thickness. A wavelength-dispersive X-ray spectroscopy (WDS) analysis identified the chemical composition of the laser cleaned surfaces for the complete set of conditions tested. It was found that low oxidation levels were attained when the laser beam was scanned at 14 kHz followed by a 6 kHz laser beam scan which is also the optimal condition for the highest material removal rate. An X-ray diffraction (XRD) analysis identified the type and magnitude of residual stresses after the laser cleaning process. The measured residual stresses are tensile in nature with an average magnitude of 547 MPa, which are comparable to those observed in laser additive processes.

Keywords: laser removal, thermal barrier coating, bond layer, MCrAlY, Inconel 718

Corresponding author's e-mail: hyzheng@simtech.a-star.edu.sg

1. INTRODUCTION

Laser surface treating of super alloys has attracted attention of the scientific community in recent years [1-17]. However, research on laser cleaning had focussed on areas such as Nd:YAG and CO_2 lasers preparation of titanium alloy components for joining by electron beam (EB) welding and diffusion bonding by Turner et al. [5-8]. Oltra and co-workers reported an enhanced oxide film removal from metal surfaces (steel substrate) by the application of pulsed laser irradiation in a liquid confinement at controlled electrochemical potential [9]. Sezer, H.K. et al. [10-12] have reported bond layer (BL) and thermal barrier coating (TBC) delamination mechanisms and the effects of a coaxial and a secondary gas jet (with different angles) on the material ejection process while drilling acute angled holes, typically found on aero-engine components, on Nickel alloys with BL/TBC coatings. Feng Q. et al. [13] employed a Ti:sapphire femtosecond laser to drill single-crystal superalloy Rene N5 through thermal barrier coatings and bond coat (MCrAlY) without defects such as delamination, recast layer or spatter. More recently, different types of lasers have been employed in selective laser sintering of Inconel 718 for three dimensional printing and repair of valuable components [14-17]. Jia and Gu investigated the effect of laser energy input in selective laser sintering of Inconel 718 which modified the microstructure, hardness and wear resistance properties of the produced elements [14]. Bennett, J. et al. found that longer cooling and solidification rates of laser deposited Inconel 718 generated coarser microstructures which reduced the ultimate tensile strength of the deposited elements [16]. The generated phases in pulsed Nd:YAG laser deposition of Inconel 718 and their effect on stress rupture behaviour of elements was reported by Sui S. et al. [17].

Modern hot section aero engine components are commonly coated with corrosion resistant and thermal barrier coatings. During an overhaul cycle, these coatings need to be removed before any repair can be performed. The coating thickness may vary due to conditions such as coating location (e.g. leading or trailing edge of a vane), tolerance in the coating thickness during the application process, diffusion of the coating during engine run and coating chip-off that may occur due to handling and engine operation.

Various methods have been proposed for the removal of TBC for turbine components including the use of shockwaves [18, 19], abrasive water jets [20-22] as well as initial explorations with lasers [23]. The current method to strip TBC and BL coatings from the aero engine components includes the combined use of abrasive blasting and acid baths. However, due to coating variation, components' shape contour, and the cooling holes configuration, employing these two methods may cause excessive wear on the parent material on some areas and leave remnant coating on other locations. Furthermore, acid stripping can also result in stress corrosion cracking and alloy depletion. Therefore, a stripping/cleaning system that is fast and able to

remove coating without affecting the base metal will be of interest for aerospace maintenance repair and overhaul industry. To this end, this research work explores for the first time, in a systematic and comprehensive experimental approach, the capability of a laser cleaning process as an alternative method for the removal of TBC coating and BL. Lasers are precise, powerful and contactless tools capable of removing almost all kinds of materials given the selection of the right wavelength, power level and temporal interaction (pulse duration). These advantages have allowed their exploration of multiple lasers on the removal of coatings, paints and contaminants from various types of metals and concrete substrates [24-26] relevant to multiple industrial applications. Moreover, computer programmable beam delivery through optical fibres combined with galvanometer-scanners and programmable focussing optics allows flexible and precise laser beam delivery over three dimensional shapes [27]. Here, the explored laser removal method aims to build a foundation for an effective and automated approach for the removal of TBC and BL coatings from aero-engine components, without introducing additional waste to the cleaning system. In this contribution, a high power Nd:YAG laser (λ=1064 nm, τ=38 ns) system is investigated to remove the TBC and BL coatings from equiaxial Inconel 718 alloy typically employed in the manufacture of aero engine components. Since laser cleaning is a thermal process, the quality criteria were based on the degree of side-effects such as surface oxidation, melting and crack development, micro-structural changes, and residual stress on the metal substrates as well as the achievable material removal rates. The effects of the high-intensity laser interaction with the Inconel 718 alloy were analysed and the findings discussed.

Different assisting media were explored to improve the material removal rate of thermal barrier coating (TBC) and the quality of the laser cleaned surfaces as well as to optimise the consumption of energy. A novel two step laser scanning method was developed for the removal of the though interfacial bond layer (BL) at competitive rates, with low oxidation level and minimal recast layer. The chemical and mechanical integrity of the laser cleaned surfaces under different process conditions were investigated through WDS and XRD analyses as well as optical and SEM microscopy inspection.

2. MATERIALS AND METHODS

A nickel base alloy equiaxial Inconel 718 coupons with chemical composition shown in Table 1 were employed in this work. This Nickel base alloy has a polycrystalline structure with fine grains given its solution annealing condition (AMS 5596). The coupons have the following dimensions 50 x 45 x 3 mm; they were thoroughly cleaned by acetone wiping and ultrasonic bath (30 minutes) to remove any contaminants from their surfaces. The coupons were first coated with 350 µm bond layer (BL) MCrAlY with a chemical composi-

TABLE 1
The chemical composition of Inconel 718 employed (in weight percent, wt%).

C	Mn	P	Si	Cr	Ni	Al	Mo	Cu	Cb	Ta	Ti	Co	B	Fe
0.05	0.08	0.005	0.05	18.26	51.72	0.62	2.89	0.04	5.04	0.01	1.01	0.38	0.003	19.83

TABLE 2
The chemical composition of bond layer coating (MCrAlY) (in weight percent, wt%).

Ni	Cr	Al	Y	Co
32	21	8	0.5	Balance
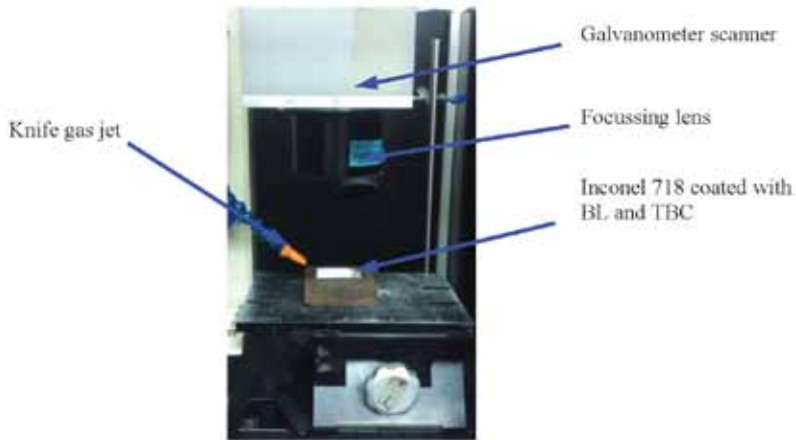
FIGURE 1
Experimental set up for the laser removal of TBC and BL (MCrAlY).

tion shown in table 2 and then coated with 1 mm Yttria-stabilised zirconia (8%). The coating method was low-pressure plasma spray (LPPS) for the bond layer, followed by a diffusion stage and finally atmosphere plasma spray (APS) for top coat (TBC).

A high-power laser beam was directed at the TBC and bond layer to cause thermal ablation and their removal. A pulsed mode Nd:YAG laser (DQ x50 S, ROFIN Baasel, GbmH) λ=1064 nm, τ=38 ns with an adjustable repetition rate of 6 – 15 kHz and maximum average power of 500 W was employed for the cleaning operation. The laser beam was delivered by a 600 μm squared core optical fibre to a collimating unit and into a galvanometer scanner. A telecentric f-theta lens (fl=80mm) focused the laser beam into a top hat square spot of 0.6 mm. Figure 1 shows the experimental set up for the multiple experiments conducted in this research work.

Multiple laser removal techniques and the application of different assisting media were explored. A parametric investigation for the removal of TBC and BL from flat samples was conducted under different pulse duration, repetition rates, laser power level, scanning patterns and speed. Furthermore, process optimisation was followed to maximise material removal rates, minimise thermal effects, and improve surface quality.

2.1. Material Characterisation

The laser removal of thermal barrier coating (TBC) was analysed by optical microscopy. The samples ablated by the laser beam were measured with an Optical Microscope (MX51, Olympus, Corp.) coupled with an image analyser software.

Metallurgical analyses were conducted to determine thermal effects, material degradation and surface quality of laser cleaned samples. The Inconel 718 coupons with the bond layer (MCrAlY) stripped by the laser ablation process were cross-sectioned and mounted on hard ceramic for grinding and polishing. An etchant solution was prepared with the composition of 15 ml hydrochloric acid (HCl), 10 ml acetic acid (CH_3COOH) and 10 ml of nitric acid (HNO_3) to analyse the grain structure on the surface irradiated by the laser beam through optical and SEM microscopy. A scanning electron microscope (SEM) (EVO50, Carl Zeiss, AG) was employed to inspect the presence of re-solidified material (recast layer thickness) through chemical etching. This system was coupled with an EDX analyser to verify the elemental composition of the recast layer. A field emission scanning electron microscope (FE-SEM) (Ultra Plus, Carl Zeiss, AG) was employed for a wavelength-dispersive X-ray spectroscopy (WDS) analysis to verify if the bond layer coating was completely removed and to measure the oxidation level present on the laser cleaned surfaces. Finally, an X-ray diffractometer (μ-X360s, Pulsetec USA, Inc.) was employed for X-ray powder diffraction (XRD) analysis to determine residual stress on the laser cleaned substrates.

2.2. Laser removal of thermal barrier coating (TBC)

Laser ablation of the TBC (Yttria-stabilised zirconia 8%) was first investigated. A series of preliminary tests identified feasible conditions to remove this material. Small areas were employed to tests various process conditions. The TBC coated coupons were sectioned into smaller test pieces. Tracks of 2 mm width by 12.5 mm length were cleaned through multiple passes of the laser beam directed by the galvanometer scanner. The laser beam movement paths were tested at 70 and 80 % overlapping. Five power levels 400, 412.5, 425, 437.5 & 450 W and two locations of the beam focal point position (i.e. at top and bottom of the TBC coating) were tested. The laser beam was scanned at 975 mm/s and 50 passes were applied in each test in a dry condition. The use of two different media i.e. Argon gas jet and low-pressure water steam was explored to analyse their effect in the laser removal process. Table 3 lists all the tests conducted.

TABLE 3

Laser process conditions tested in the removal of thermal barrier coating - TBC - (Yttria-stabi-
lised zirconia 8%).

Test No.	Condition	Beam overlap (%)	Focal point position (mm)	Power level (W)
1	Dry	70	0	400
2	Dry	70	0	412
3	Dry	70	0	425
4	Dry	70	0	437
5	Dry	70	0	450
6	Dry	70	-1	400
7	Dry	70	-1	412
8	Dry	70	-1	425
9	Dry	70	-1	437
10	Dry	70	-1	450
11	Dry	80	0	400
12	Dry	80	0	412
13	Dry	80	0	425
14	Dry	80	0	437
15	Dry	80	0	450
16	Dry	80	-1	400
17	Dry	80	-1	412
18	Dry	80	-1	425
19	Dry	80	-1	437
20	Dry	80	-1	450
21 - 30	Argon gas	75	0, -1	400, 412,425, 437 450
31 - 40	Water steam	75	0, -1	400, 412,425, 437 450

The trials with assisting media followed similar conditions differing only on the
laser beam overlap at 75%. A diagram of the sample sectioning and the various
conditions tested to assist the removal of the TBC coating are shown in figure
2. The conditions investigated included dry ablation of TBC, the use of an
assisting Argon gas jet and the application of a low-pressure water steam jet.
The complete removal of the coating, under various conditions, was verified
through optical microscopy. The area of removed TBC coating was measured
at the cross section of all laser ablated samples and the total volume of removed
material was computed. The expenditure of energy was then calculated from
the process parameters. An energy consumption was computed from all condi-
tions tested by the following equation:
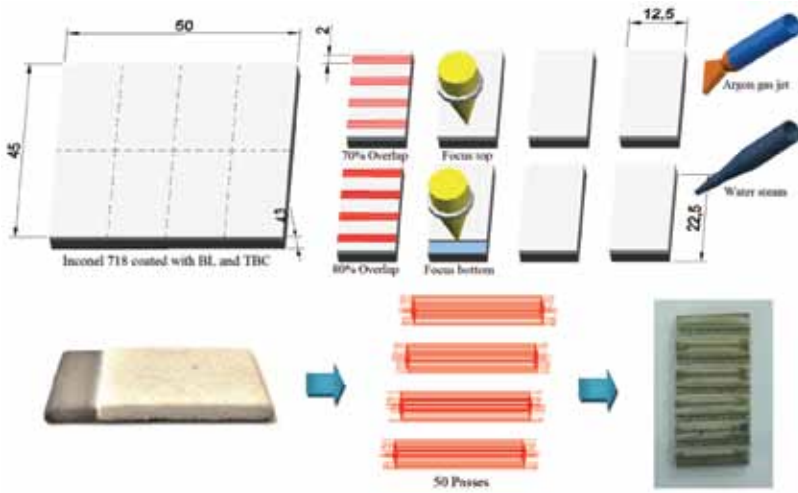
FIGURE 2
Laser removal of thermal barrier coating (TBC) of 1 mm thickness following 70 & 80% laser beam overlap, beam focus on top & bottom of the TBC layer, dry ablation, with assisting Argon gas jet, and with a low-pressure water steam jet. Clean tracks of 2 x 12.5 mm were obtained after 50 passes of the laser beam.

$$EC = \frac{P * t}{V_m} \tag{1}$$

Where EC is the energy consumption (J/mm^3), P is the average power (W), t is the total processing time (s), and V_m is the volume of material removed (mm^3).

2.3. Laser removal of the bond layer (BL)

Laser cleaning experiments were conducted on Inconel 718 coupons coated with bond layer (BL) coating MCrAlY. High material removal rate and minimal thickness of the recast layer formed on top of the laser cleaned surface were targeted. The measured thickness of the BL coating was on average 350 μm. The laser beam was scanned on top of the BL to form a 2 x 12.5 mm clean track with a 70 % beam overlapping at four different power levels and under four different frequencies. Multiple preliminary tests have shown that higher material removal rates result when delivering the laser beam at high frequency; however, excessive melting develops which yields a non-uniform surface and left behind thick recast layers. On the other hand, delivering the laser at the low frequency generated flat uniform surfaces, but the material removal rates were very low and the heat input on the pieces was very high. Therefore, a novel laser removal process of this hard to process coating was implemented by applying two sets of laser scans. The first set was delivered

TABLE 4

Laser process conditions tested in the removal of bond layer - BL - (MCrAlY), following a two-step laser removal process. In the first step, the laser beam is scanned at high pulse frequency (≥8 kHz) with different number of passes (~215 passes). In the second step, laser beam is scanned at low frequency (6 kHz) with 100 passes.

No.	Beam overlap (%)	Focal point position (mm)	First removal step		Second removal step	
			Frequency (kHz)	Power level (W)	Frequency (kHz)	Power level (W)
1	70	0	8	315	6	315
2	70	0	8	360	6	315
3	70	0	8	405	6	315
4	70	0	8	450	6	315
5	70	0	10	315	6	315
6	70	0	10	360	6	315
7	70	0	10	405	6	315
8	70	0	10	450	6	315
9	70	0	12	315	6	315
10	70	0	12	360	6	315
11	70	0	12	405	6	315
12	70	0	12	450	6	315
13	70	0	14	315	6	315
14	70	0	14	360	6	315
15	70	0	14	405	6	315
16	70	0	14	450	6	315

at high frequency (≥8 kHz) which increased the material removal rate and the second delivers the laser beam at low frequency (6 kHz) which flattened the cleaning track and reduced the recast layer thickness.

In order to identify which combination of frequencies is ideal for the laser removal of this bonding layer a comprehensive experimental work was conducted. Here, two sets of laser beam scans were applied in each test. The first scan set comprised a large number of passes (on average 215) of the laser beam at four different frequencies i.e. 8,10,12 & 14 kHz, following four power levels (315, 360 405 & 450W) and under different traverse speeds and the number of laser scans. This initial set of passes at a high frequency removed the bulk of the BL coating material. A second scan set comprised 100 passes of the laser beam at 6 kHz frequency and average power of 315 W i.e. 70% of the power available in this laser system at this frequency. This secondary set of passes flattened the surface of the clean track and reduced the thickness of the recast layer as indicated above. Table 4 list the combina-
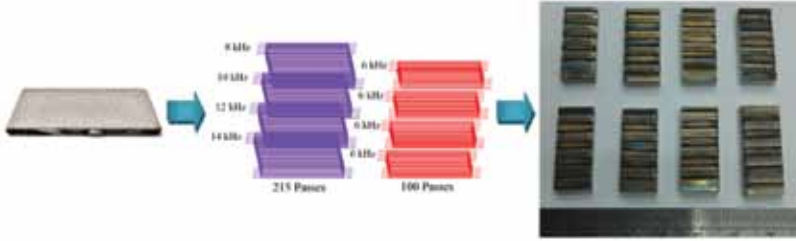
FIGURE 3

Laser removal of bond layer (BL) coating MCrAlY of 350 μm thickness at 70% laser beam overlap, focusing on top of the BL layer following two sets of laser scans, first a set of ~ 215 passes at different frequencies 8,10,12 & 14 kHz each followed by a second set of 100 passes at 6 kHz.

tion of process parameters tested for the removal of bond layer. A schematic of the laser removal procedure followed to remove the BL coating is shown in figure 3.

3. RESULTS

3.1. Beam overlap effect in laser removal of thermal barrier coating (TBC)

The laser cleaning of TBC with 80% beam overlapping produced clean tracks for the power levels and focal point positions tested under 50 passes of the laser beam. In contrast, at 70% laser beam overlap under the same process conditions did not completely remove the TBC coating. The consumption of energy per unit of volume of TBC removed was calculated for all the conditions tested in this experiment following equation 1. At 70% percent laser beam overlap, the effect of the focal point position on the energy consumption was minimal yielding only on average 1.64% lower energy consumption when the beam was focused at the bottom of the TBC coating as shown in figure 4 (b & d). The longer interaction time at 80% overlapping condition yielded higher energy consumption. A similar trend was observed when increasing the power applied in the removal process. Here, the laser beam focused at the bottom of the TBC layer improved on average 6.33% the energy consumption efficiency as shown in figure 4 (a & c). This, as the laser beam is converging along the depth of the TBC coating layer, which maximises the removal of material in the laser cleaning process.

3.2. Beam focal point location and assisting media effect in laser removal of thermal barrier coating (TBC)

The effect of focusing the laser beam on the top and bottom of the TBC coating layer was investigated for a laser beam overlapping of 75% at different power
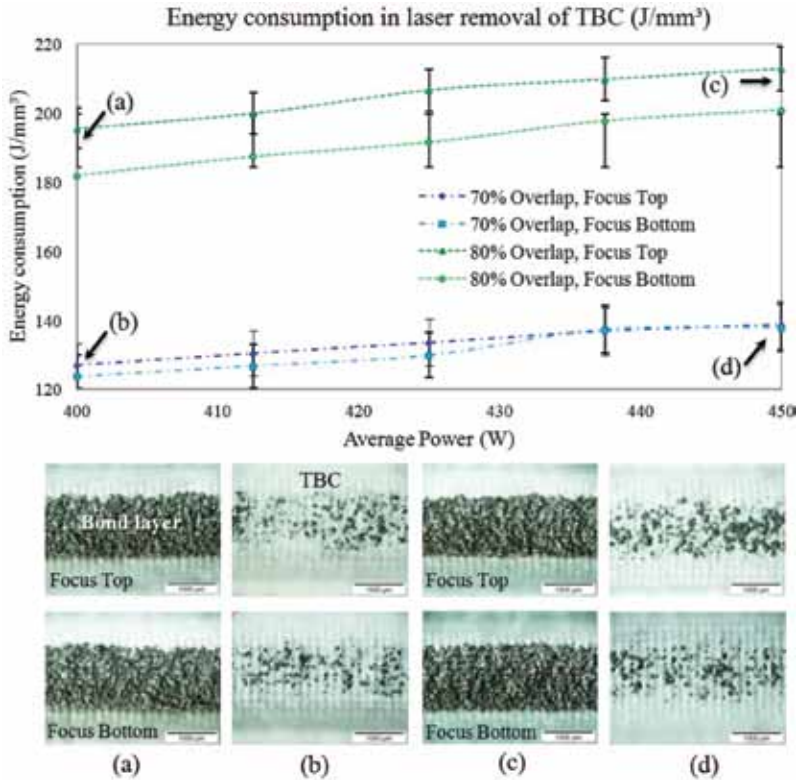
FIGURE 4

Calculated energy consumption in the laser cleaning of TBC at different beam overlapping conditions, power level, and focal point positions. Clean tracks were obtained at 80% beam overlapping at 400W (a) and 450W (c) power levels. Tests at 70% beam overlap showed remnants of TBC coating at 400 W (b) and 450 W (d) power levels.

levels in a definitely manner. Since the two previous conditions tested resulted in excessive removal (80% overlap) or incomplete removal (70% overlap) of the TBC coating layer. Furthermore, the effects of assisting media in the laser cleaning process were explored for the focal point position at the bottom of the TBC coating layer. In particular, the shear stress produced by an assisting side Argon knife gas jet at 2 bars of pressure with an incident angle of ~ 25° and the explosive ejection of steam water while in interaction with the laser beam were investigated. In these experiments, five different power levels were employed, while maintaining constant the scanning speed of 975 mm/s, the overlapping of the scanned lines was set at 75%, and the number of passes at 50 for each condition (see Table 3 tests 21-40). The energy consumption per unit of volume in laser cleaning of TBC for each condition tested was calculated following equation 1. A graphical overview of the results obtained in this experiment is presented in figure 5. The effect of the beam focal point position was clearly observed at a 400W
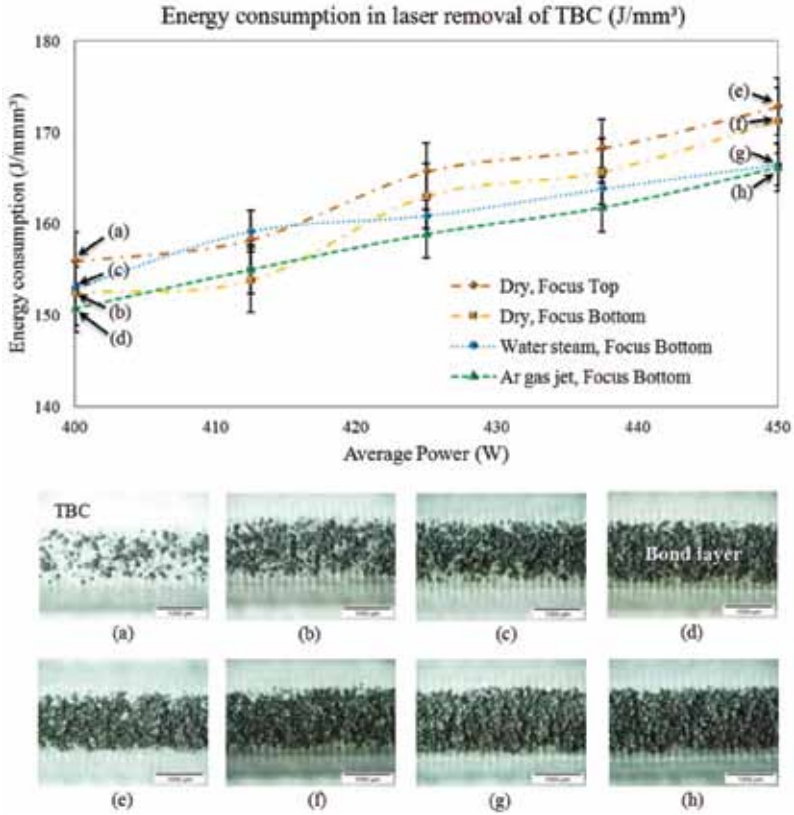
FIGURE 5
Calculated energy consumption in the laser cleaning of TBC at 75 % overlapping and at different focal point positions and assisting media. Dry TBC with laser beam focused on top at 400W (a) and 450W (e); Dry TBC with laser beam focused at the bottom at 400W (b) and 450W (f); Water steam with laser beam focused at the bottom at 400W (c) and 450W (g); Argon gas jet with laser beam focused at the bottom at 400W(d) and 450W (h).

power level at the dry condition which generated cleaner tracks when focusing at the bottom figure 5(b) as compared to focussing at the top figure 5(a). In general, higher power level produced clean tracks as seen in figure 5 (e - h), while the action of the Argon gas jet figure 5(d) and low-pressure water steam figure 5(c) helped to obtain cleaner tracks than those obtained by the laser beam alone -dry condition- figure 5(b). High power level, however, increased the amount of energy consumed per unit volume as shown in the graph in figure 5.

3.3. Laser removal of bond layer
Multiple experiments were conducted at each of the 16 combinations matching four power levels (315, 360 405 & 450W) with four pulse frequencies (8,
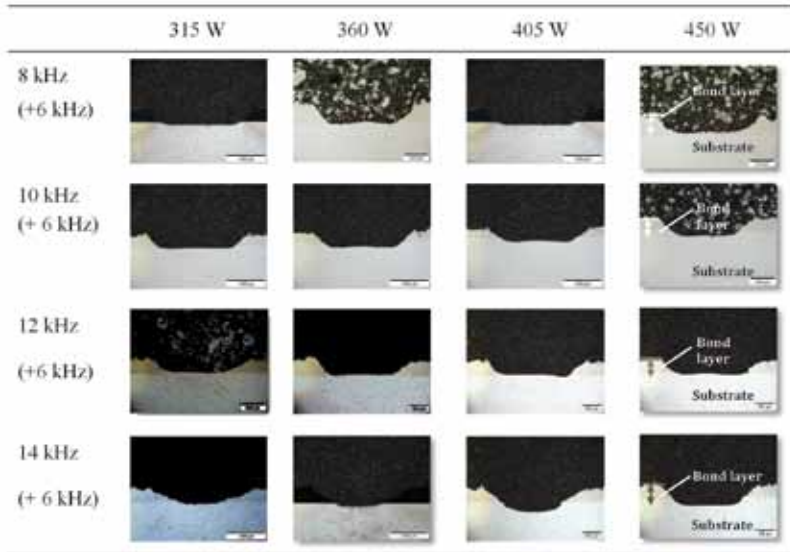
FIGURE 6

Laser removal of the bond layer by two sets of scanning patterns (two different frequencies) with 70 % overlapping of the laser beam and different power levels, traverse speed and number of passes.

10, 12 & 14 kHz) to reach the substrate with flat surfaces, avoiding cracks and obtaining thin recast layers (see Table 4). The traverse speed and number of laser beam passes were adjusted to obtain clean pieces with these combinations of pulse frequencies. Figure 6 shows the cross-section of the BL laser removal results for all the combinations investigated. The samples show that the BL was completely removed where the laser beam reached the substrate and the cleaned tracks had fairly flat surfaces.

The material removal rate was measured for each parameter combination. The thickness of the recast layer left on the surface after the laser stripping of the BL for each condition was measured by optical microscopy. Figure 7 shows both the computed material rate and the thicknesses of the recast layer measured after the laser stripping process for all the conditions. The recast layer thicknesses recorded were below 5 μm in all conditions.

The experimental results show that low frequencies of 8 & 10 kHz, at similar power levels, yielded lower material removal rates as compared to higher frequencies of 12 & 14 kHz, which improved the rate of material removal. The second laser beam scan set of 100 passes at 315W average power and 6 kHz pulse frequency which yields higher peak power. This second scan flattens the treated surface by the laser beam. The high peak power ablates the material uniformly; however, the material removal rate is low and the heat input is high.
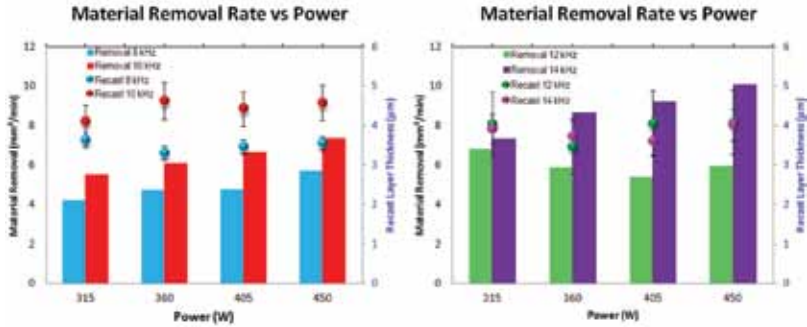
FIGURE 7
Material removal rate and recast layer thickness in the laser removal of BL (MCrAlY) by two scanning sets at different frequencies.

3.4. WDS Analysis of laser cleaned surfaces

A Wavelength-Dispersive X-Ray Spectroscopy (WDS) analysis of the laser stripped surfaces was conducted to determine the oxygen content after the cleaning process (reduction or avoidance of oxidation effects). The analysis was conducted on the cross section of the laser treated surfaces. The WDS analysis reveals the chemical composition of the recast layer and the substrate material Inconel 718 for the complete experimental matrix on BL laser cleaning. The analysis identified the proportion of the main elements present in Inconel 718 and the bond layer coating MCrAlY. Here, twelve elements were analysed at four points in each recast layer cross section. Furthermore, two points on the base material for half of the treatments were analysed as shown in Figure 8. The best results obtained in terms of low levels of Oxygen were obtained when cleaning with laser frequencies of 8 and 14 kHz. Table 5 shows the elements detected by the WDS analysis of this selected laser cleaned surfaces. The second condition at 14 kHz is beneficial for this process as it resulted in higher removal rates of the bond layer.

3.5. XRD Analysis

An X-ray diffraction (XRD) analysis was conducted to identify the residual stresses present in laser cleaned surfaces. This technique has been employed by various groups to investigate the degree of change to the residual stresses in the sample after subjecting the sample to TBC depositions and cyclic thermal treatments [28-31]. The residual stress analysis was conducted with an X-ray diffractometer following the cosα method. The diffractometer employs a Chromium X-ray source. The scanning angle was fixed at 35°, while X-rays were collimated by a 1mm point collimator. Four measurements were taken from the sample surface, each point located 3 mm apart. Figure 9 shows the set up employed for this analysis. The results indicated that tensile stresses
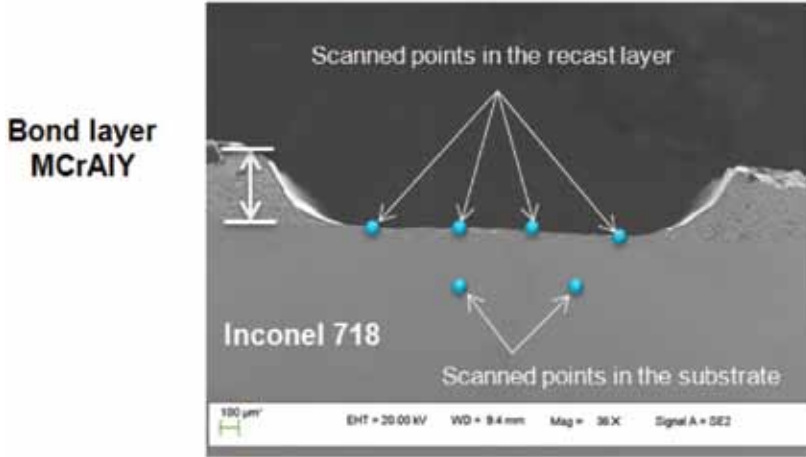
FIGURE 8
WDS analysis conducted at four locations on the recast layer cross-section and at two locations on the substrate.

TABLE 5
Selected WDS results of laser cleaned surfaces at 8 and 14 kHz.

FREQ	Element (weight %)	Recast layer				Inconel 718	
		315 W	360 W	405 W	450 W	360 W	405 W
8 kHz	Ni	55.56	51.74	50.66	54.91	50.81	50.63
(+ 6 kHz)	Co	2.77	2.11	0.79	1.25	0.43	0.40
	Fe	19.15	18.24	18.28	19.09	18.64	18.66
	Cr	12.93	13.16	14.00	10.85	17.86	18.25
	Mo	2.30	2.42	2.48	2.37	2.91	2.23
	O	1.21	1.17	2.29	1.79	0.84	0.89
	Al	0.85	1.14	1.00	1.00	1.64	1.70
14 kHz	Ni	50.97	49.83	52.23	51.72	50.94	50.48
(+ 6 kHz)	Co	0.70	1.43	1.70	5.53	0.36	0.38
	Fe	17.50	16.69	17.26	16.12	18.55	18.29
	Cr	9.94	10.69	9.99	10.26	18.21	18.25
	Mo	3.57	3.15	3.23	2.50	2.86	2.80
	O	3.15	2.81	2.99	2.01	0.79	0.74
	Al	0.91	1.74	1.30	1.74	1.77	1.77

were present on the surface of the laser cleaned samples as shown in Table 6, with an average value of 547 MPa. Conversely, compressive stresses of an average value of -264 MPa were measured from the surface of a pristine cou-
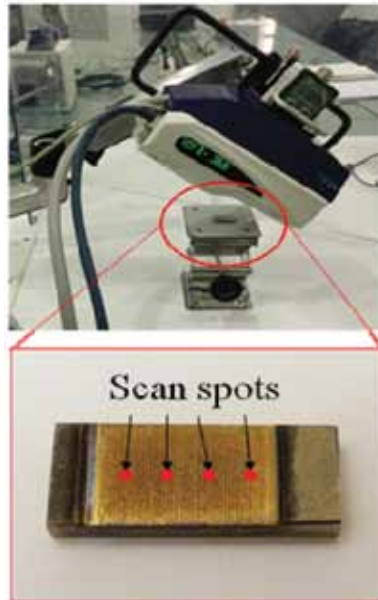
FIGURE 9
Set-up for XRD analysis of a laser treated Inconel 718.

TABLE 6
Residual stress (MPa) measurements of Inconel 718, Inconel 718 coated with BL and TBC and a laser ablated Inconel 718.

Inconel 718	Inconel + BL + TBC	Laser cleaned Inconel 718
-358	975	347.2
-154	269	456
-361	302	921.2
-183	706	465.5

pon. Finally, tensile stresses of an average value of 563 MPa were measured from samples subjected to TBC coating process conditions. This residual stresses balance between the substrate/coating compound results from quenching stresses and the coefficient of thermal expansion (CTE) mismatch stress [28-32]. The former develops when the melted TBC coating (Yttria-stabilised zirconia) rapidly solidifies and cools over the substrate material (Inconel 718 + BL) [28, 29]. The latter -CTE- results from the thermal expansion mismatch between the coating materials and the substrates [30, 31]. The similar average values of residual stresses obtained from both the TBC coated and the laser cleaned samples suggest that the laser cleaning process does not

induce significant changes to the surface residual stress profile of the sample. Tensile stresses were expected on this process as the Inconel 718 substrates were heated by the laser removal process which then follows a cooling process. These phenomena have been reported on laser additive processes [33].

4. DISCUSSION

4.1. Laser removal of the thermal barrier coating

From the experimental evidence reported herein, it was observed that the focal point position at the bottom of the TBC coating yielded cleaner tracks as the laser beam converges along the thickness of the coating. Here, the power density continuously increases given the smaller beam spot sizes. The opposite effect is observed when the focal point position is located at the top of the TBC i.e. the laser beam starts to diverge as it propagates along its thickness. Furthermore, the consumption of energy was better optimised when the laser beam was located at the bottom of the TBC coating layer.

The use of assisting Argon gas jet helped to clean tracks and to reduce the energy consumption see figure 5 (d & h). This by ejecting more material from the processing area given the shear stress applied to it, this clearing effect also enhances the laser-material interaction. Furthermore, water steam also reduced the energy consumption per unit of material removed. This by expelling more material from the cleaned surfaces through an explosive boiling effect produced when the low-pressure water steam jet interacts with the high-power infrared laser beam. Optimal removal conditions were power level 400 - 450W, laser beam overlap of 75%, focus at the bottom of the TBC layer, 50 passes and 975 mm/s traverse speed. These conditions yielded clean traces with average removal rates of 140 mm³/min.

A novel two-step laser scanning process removed the BL (MCrAlY) coating which is a very tough interface protective layer for the Inconel 718 alloy. This layer proved difficult to be removed by a single set of parameters, therefore a suitable method has been developed. The combination of different scanning sets proved effective for the laser cleaning process of the BL coating. Here, the scanning of the laser beam at high pulse frequencies improves the removal rate of the material. The application of a second scanning set, i.e. laser beam delivered at low frequency and high-power level (high peak power), flattened the surface of the laser cleaned sample and yielded thinner recast layer. This layer cannot be fully avoided as the thermal nature of the nanosecond laser removal process; nonetheless, it was minimised as it was below 5 µm in thickness in all conditions. The optimal condition identified was a set of 170 passes at 14 kHz frequency and 450W (100% of power level available). This was followed by a set of 100 passes at 6 kHz and 315W yielding a material removal rate of 10 mm³/min and recast layer of 4 µm.

A WDS analysis was employed to identify the chemical composition of laser cleaned surfaces for the complete set of conditions tested. Since the laser removal process is conducted in an open-air environment and under high power level condition, the Nickel based alloy is susceptible to oxidation. It is important to minimise any oxidation as Inconel 718 is employed in the manufacture of valuable elements such as aero-engine and power turbine components. In particular, serviced aero-engine components follow a series of repairs and coating steps after the cleaning process of TBC and BL; therefore, oxidation levels shall be minimised. Results from WDS analysed laser treated materials showed that low oxidation levels were attained in pieces cleaned by the laser beam scanned at 8 kHz and at 14 kHz followed by 6 kHz scanning step. The latter combination i.e. 14 kHz followed by 6 kHz laser beam scans at 400W power level was the optimal condition as it yielded higher removal rate of the material.

5. CONCLUSIONS

A laser removal process of TBC was conducted with a high power Nd:YAG pulsed laser. Clean tracks were obtained at 75 & 80% overlapping of the top-hat and 600 μm square laser beam employed. The efficiency of the laser cleaning process improved when the focus was located at the bottom of the TBC coating as the laser beam converges along its thickness. The assisting media, Argon gas jet and low-pressure steam water, improved the material removal rate in the TBC laser cleaning process which in turn reduced the consumption of energy.

A novel two step laser removal process of the bond layer (MCrAlY) has been developed. The first step delivered multiple passes of the laser beam at high pulse frequency (14 kHz) which achieved high material removal rate. The second step consisted of a set of multiple passes of the laser beam at low pulse frequency which flattened the cleaned sample surface and yielded thinner recast layer.

WDS analysis was employed to identify oxidation levels on BL laser cleaned samples. A laser removal process with 170 passes of the laser beam at pulse frequency of 14 kHz at 450W, followed by 100 passes of the laser beam at pulse frequency of 6 kHz at 315W was found as optimal condition as it yielded higher material removal rate with low oxidation at the surface.

XRD analysis helped to identify the type and magnitude of residual stresses after the laser cleaning process. Their measured residual stresses are tensile in nature with an average magnitude of 547 MPa, which were comparable in magnitude to the tensile stresses from samples subjected to the TBC coating process at 563 MPa. The pristine Inconel 718 coupons had compressive residual stress with average value of -264 MPa.

REFERENCES

[1] Guan Y.C., Ng G. K. L., Zheng H. Y., Hong M. H., Hong M.H., Hong X. and Zhang Z. Laser surface cleaning of carbonaceous deposits on diesel engine piston. *Applied Surface Science* **270** (2013), 526-530.

[2] Wang X. and Zheng H. Picosecond laser micro-drilling, engraving and surface texturing of tungsten carbide. *Journal of Laser Applications* **30** (2018), 032203.

[3] Wang X.C., Wang B., Xie H., Zheng H.Y. and Lam Y.C. Picosecond laser micro/nano surface texturing of nickel for superhydrophobicity. *Journal of Physics D: Applied Physics* **51** (2018), 115305.

[4] Lu L., Zhang Z., Guan Y. and Zheng H. Comparison of the effect of typical patterns on friction and wear properties of chromium alloy prepared by laser surface texturing. *Optics & Laser Technology* **106** (2018), 272-279.

[5] Turner M.W., Crouse P.L. and Li L. Comparison of mechanisms and effects of Nd:YAG and CO2 laser cleaning of titanium alloys. *Applied Surface Science* **252** (2006), 4792-4797.

[6] Turner M.W., Crouse P., Li L. and Smith A. J. E. Investigation into CO_2 laser cleaning of titanium alloys for gas-turbine component manufacture. *Applied Surface Science* **252** (2006), p. 4798-4802.

[7] Turner M.W., Crouse P. and Li L. Comparative interaction mechanisms for different laser systems with selected materials on titanium alloys. *Applied Surface Science* **253** (2007), 7992-7997.

[8] Whitehead D.J., Crouse P.L., Schmidt M.J.J., Li L., Turner M.W. and Smith A.J.E. Monitoring laser cleaning of titanium alloys by probe beam reflection and emission spectroscopy. *Applied Physics A* **93** (2008), 123-127.

[9] Dahl K.V., Hald J. and Horsewell A. Interdiffusion between Ni-based superalloy and MCrAlY coating. *Defect and Diffusion Forum* **258-260** (2006), 73-78.

[10] Sezer H.K., Pinkerton A.J. and Li L. An investigation into delamination mechanisms in inclined laser drilling of thermal barrier coated aerospace superalloys. *Journal of Laser Applications* **17** (2005), 225-234.

[11] Sezer H.K., Li L., Schmidt M., Pinkerton A.J., Anderson B. and Williams P. Effect of beam angle on HAZ, recast and oxide layer characteristics in laser drilling of TBC nickel superalloys. *Machine Tools & Manufacture* **46** (2006), 1972-1982.

[12] Sezer H.K., Li L. and Leigh S. Twin gas jet-assisted laser drilling through thermal barrier-coated nickel alloy substrates. *International Journal of Machine Tools & Manufacture* **49** (2009), 1126-1135.

[13] Feng Q., Picard Y., McDonald J. P., Rompay V.P.A., Steven Y. and Pollock T. M. Femtosecond laser machining of single-crystal superalloys through thermal barrier coatings. *Materials Science and Engineering A* **430** (2006), 203-207.

[14] Jia Q. and Gu D. Selective laser melting additive manufacturing of Inconel 718 superalloy parts: Densification, microstructure and properties. *Journal of Alloys and Compounds* **585** (2014), 713-721.

[15] Wang D., Tian Z., Shen L., Liu Z. and Huang Y. Effects of laser remelting on microstructure and solid particle erosion characteristics of ZrO_2–7wt% Y_2O_3 thermal barrier coating prepared by plasma spraying. *Ceramics International* **40** (2014), 8791 - 8799.

[16] Bennetta J. L., Kafka O. L. Liao H. Wolff S. J. Yu C. Cheng P. Hyatt G. Ehmann K. Cao J. Cooling rate effect on tensile strength of laser deposited Inconel 718. *Procedia Manufacturing* **26** (2018), 912-919.

[17] Sui S., Chen J., Ma L., Fan W., Tan H., Liu F. and Lin X. Microstructures and stress rupture properties of pulse laser repaired Inconel 718 superalloy after different heat treatments. *Journal of Alloys and Compounds* **770** (2019), 125-135.

[18] Helmick D.A. and Burin D.L. Thermal barrier coating removal via shockwaves stresses, *T.U.S.P.a.T. Office*, Editor. 2010, General Electric Company: USA. 4.

[19] Helmick D.A. and Burin D. A. Method and system for removing thermal barrier coating, *T.U.S.P.a.T. Office*, *Editor*. 2010, General Electric Company: USA. 6.

[20] Thompson C.E. Water jet stripping and recontouring of gas turbine buckets and blades*, T.U.S.P.a.T. Office,* General Electric Company: USA. 13.

[21] Miller M.O., Pearson W. R. and Thompson W. R. Method and apparatus for removing coatings from a substrate using multiple sequential steps, *T.U.S.P.a.T. Office*, Editor. 2011, Huffman Corporation: USA. 9.

[22] Thompson W.R. Method and apparatus for selectively removing portions of an abradable coating using a water jet, *T.U.S.P.a.T. Office, Editor.* 2010, Huffman Corporation: USA. 9.

[23] Marimuthu S., Kamara A. M., Sezer H., Li L. and Ng G.K.L. Numerical investigation on laser stripping of thermal barrier coating. *Computational Materials Science* **88** (2014), p8.

[24] Wolf K. Laser Strip: A Portable Hand-Held Laser Stripping Device for Reducing VOC, *Toxic and Particulate Emissions*. 2009: California, USA. 129.

[25] Li L., Spencer J. T. and Key P. H. A comparative study of the effects of laser wavelength on laser removal of chlorinated rubber. *Applied Surface Science* **138-139** (1999), 418-423.

[26] Razab M.K.A.A., Noor A.M., Jaafar S.M., Abdullah N. H., Suhaimi F.M., Mohamed M., Adam N., Alnur N. and Yusuf A. N. A review of incorporating Nd:YAG laser cleaning principal in automotive industry. *Journal of Radiation Research and Applied Sciences* **11**(4) (2018), 393 - 402.

[27] Jaeschke P. Laser cutting for carbon fiber-reinforced composite structures, in Industrial Laser Solutions for Manufacturing. PennWell: Nashua, NH, USA. 28.

[28] Levit M., Grimberg I., and Weiss B. Z. Residual stresses in ceramic plasma-sprayed thermal barrier coatings: measurement and calculation. *Material Science and Engineering* **A206** (1996), 30-38.

[29] Kesler O., Matejicek J., Sampath S., Suresh S., Gnaeupel-Herold T., Brand P.C. and Prask H. J. Measurement of residual stress in plasma-sprayed metallic, ceramic and composite coatings. *Materials Science and Engineering* **A257** (1998), 215-224.

[30] Teixeira V., Andritschky M., Fischer W., Buchkremer H.P.D. and Stöver D. Effects of deposition temperature and thermal cycling on residual stress state in zirconia-based thermal barrier coatings. *Surface and Coatings Technology* **120-121** (1999), 103-111.

[31] Teixeira V., Andritschky M., Fischer W., Buchkremer H.P.D. and Stöver D. Analysis of residual stresses in thermal barrier coatings. *Journal of Materials Processing Technology* **92-93** (1999), 209-216.

[32] Swank W.D., Gavalya R.A., Wright J.K. and Wright R.N. Residual Stress Determination from a Laser-Based Curvature Measurement, in *Thermal Spray 2000: Surface Engineering via Applied Research*, C.C. Berndt, Editor. ASM International: Montreal, Quebec, Canada. 2000, p. 7.

[33] Kamara A.M., Marimuthu S. and Li L. A numerical Investigation into residual stress characteristics in laser deposited multiple layer waspaloy parts. *Journal of Manufacturing Science and Engineering* **133** (2011), 031013-1 - 9.